Synthesis and Characterization of a New Class of Nematic Photoluminescent Oxadiazole-Containing Polyethers

ARTICLE *in* MACROMOLECULES · JULY 2003

Impact Factor: 5.8 · DOI: 10.1021/ma034382f

8 AUTHORS, INCLUDING:

Domenico Acierno
University of Naples Federico II
343 PUBLICATIONS **3,582** CITATIONS
SEE PROFILE

Salvatore Bellone
Università degli Studi di Salerno
69 PUBLICATIONS **430** CITATIONS
SEE PROFILE

Simona Concilio
Università degli Studi di Salerno
53 PUBLICATIONS **528** CITATIONS
SEE PROFILE

Alfredo Rubino
Università degli Studi di Salerno
66 PUBLICATIONS **531** CITATIONS
SEE PROFILE

Synthesis and Characterization of a New Class of Nematic Photoluminescent Oxadiazole-Containing Polyethers

Domenico Acierno,[†] Eugenio Amendola,[‡] Salvatore Bellone,[§] Simona Concilio,[⊥] Pio Iannelli,*[,⊥] Heinrich-Christoph Neitzert,[§] Alfredo Rubino,[∥] and Fulvia Villani[∥]

Dipartimento di Ingegneria dei Materiali e della Produzione, Università di Napoli, P.le Tecchio, I-80125 Napoli, Italy, Institute for Composite Materials and Biomaterials (IMCB)- CNR, P.le Tecchio, I-80125 Napoli, Italy, Dipartimento di Ingegneria Elettronica, Università degli Studi di Salerno, via Ponte Don Melillo, I-84084 Fisciano (Salerno), Italy, Dipartimento di Ingegneria Chimica ed Alimentare, Università degli Studi di Salerno, via Ponte Don Melillo, I-84084 Fisciano (Salerno), Italy, and ENEA C.R. Portici, v. Vecchio Macello - loc. Granatello, 80055 Portici (Na), Italy

Received March 26, 2003; Revised Manuscript Received June 9, 2003

ABSTRACT: The synthesis and the characterization of a new class of segmented polyethers (**PO**) containing the oxadiazole unit are reported. Because of the anisotropic shape of oxadiazole-conjugated segment, the copolymers of the series show the monotropic nematic phase to be somewhat different from that observed in the case of the low molecular mass analogous compounds. In that case, high ordered liquid crystalline smectic phases are reported while the nematic phase is observed just in few cases. According to previous reports on oxadiazole-containing materials, **PO** show high photoluminescence activity in the blue region of the visible spectra. The good solubility in chlorinate solvents allows the preparation of films with homogeneous thickness by spin coating. A glass transition temperature in the range 100−120 °C ensures good stability of film morphology at room temperature. For these features, polymers **PO** are potential candidate materials for fabricating blue-light-emitting devices.

1. Introduction

In the last few years, new polymeric materials have been synthesized and investigated for applications in the field of organic light-emitting devices (OLEDs).[1−31] For fabricating a LED, it is usually required to have the presence of very thin layers of both hole-transporting and electron-transporting molecules. The two layers are confined between a hole-injection electrode and a low work function electron-injection metal contact, respectively. Photoemission is induced by the reciprocal combination of holes and electrons at the interface, under the action of a suitable potential difference.

Polymers may be easily processed to thin stable films by the spin-coating technique, which results in a fast and versatile fabrication of devices. Moreover, chemical architecture can be set up in order to promote the specific required morphology of samples, when coupled with a suitable thermal treatment. For applications in the field of OLEDs, special polymeric materials can be synthesized by inserting along or attaching side to the chain short conjugated frames with electroluminescent properties.

We have recently shown that new oxadiazole-containing low molecular mass compounds are blue-photolumiscent materials,[32] in agreement with that reported by several authors for similar molecules.[19,24−31] We observed that the anisotropic shape of the conjugated unit promotes the appearing of high ordered smectic phases and, only in a few cases, of the nematic phase. The liquid crystalline (LC) order is particularly interesting when optical active systems are required to be anisotropic at the macroscopic level.

In this paper, we report on the synthesis and the characterization of a new class of LC photoluminescent segmented polymers having the formula **PO(*m*,*a*)**.

The insertion of the flexible aliphatic segments along and side attached to the chain moderates melting temperature and promotes solubility in organic solvents and the appearing of the nematic phase. The photoluminescence properties of polymers are also discussed.

2. Experimental Section

2.1. Materials. All reagents and solvents were purchased from Aldrich and Carlo Erba. *N*,*N*-Dimethylacetamide (DMAc) and *N*,*N*-dimethylformamide (DMF) were refluxed on calcium hydride, distilled in a vacuum, and stored on 4 Å molecular sieves. Other reagents were used without further purification. According to Scheme 1, 4,4′-dicarboxy-1,*n*-diphenoxyalkane dimethylester (**2**) and *n*-alkoxyterephthalic acid (**1**), with its chlorinated derivative (**3**), were synthesized according to a procedure previously reported.[32,33]

4,4′-Dicarboxy-1,*n*-diphenoxyalkane Dihydrazides (4). 4,4′-Dicarboxy-1,*n*-diphenoxyalkane dimethylester **2** was prepared according to the procedure described in ref 33. Compound **4** was synthesized from compound **2** reacting with an excess of hydrazine monohydrate in ethanol solution. The procedure was the following: approximately 15 g of **2** was stirred in boiling hydrazine monohydrate (160 mL) with absolute ethanol (280 mL) for 4 h. At the end, the reaction system was cooled, and the white crystalline dihydrazide **4** precipitated from the reaction solution. The solid was recovered by filtration, repeatedly washed with cold ethanol, and dried under vacuum at 60 °C. Final yields ranged between 80 and 90%. For 4,4′-dicarboxy-1,6-diphenoxyalkane dihydrazide: $T_{solid-solid} = 172.7$ °C, $\Delta H_{solid-solid} = 11.8$ J/g; $T_m = 192.0$ °C, $\Delta H_m = 215.7$ J/g. For 4,4′-dicarboxy-1,12-diphenoxyalkane dihydrazide: $T_m = 214.0$ °C, $\Delta H_m = 179.4$ J/g.

* Corresponding author. Fax: +39 089 964 057. E-mail: piannelli@unisa.it.
[†] Dipartimento di Ingegneria dei Materiali e della Produzione, Università di Napoli.
[‡] Institute for Composite Materials and Biomaterials (IMCB)-CNR.
[§] Dipartimento di Ingegneria Elettronica, Università degli Studi di Salerno.
[⊥] Dipartimento di Ingegneria Chimica ed Alimentare, Università degli Studi di Salerno.
[∥] ENEA C.R. Portici, v. Vecchio Macello - loc. Granatello.

10.1021/ma034382f CCC: $25.00
Published on Web 07/24/2003

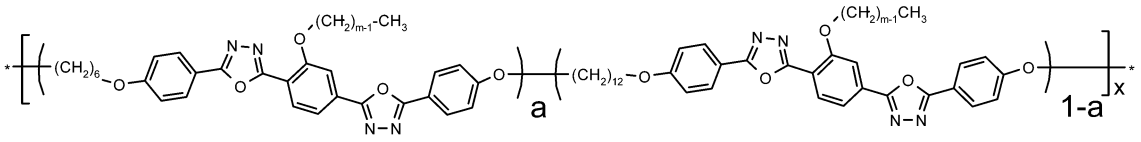

PO(m,a) m = 5, 8 a = 0, 0.5, 1

Polymer Synthesis (See Scheme 1). Step 1: To a suspension of 4,4′-dicarboxy-1,*n*-diphenoxyalkane dihydrazide (**4**) (5.00×10^{-3} mol) in dry DMAc (50 mL) at room temperature, the stoichiometric amount of the appropriate *n*-alkoxyterephthalic dichloride (**3**) was added and the reaction was allowed to take place overnight under stirring. The reaction mixture was then poured into cold water and the resulting solid product was filtered and washed twice with water. The resulting polyazide **PI** was collected with a final yield of 58−60%, purified by dissolving in boiling DMAc (30 mL) and DMF (20 mL) and subsequent precipitation with water. The final product was used in the subsequent intramolecular cyclization reaction. The proton resonance data are in agreement with the expected values. For example, **PI(8,0.5)** ($CDCl_3/CF_3$-COOD): δ (ppm) = 8.33 (d, 1H), 7.88 (d, 4H), 7.68 (s, 1H), 7.62 (d, 1H), 7.08 (d, 4H), 4.38 (t, 2H), 4.15 (m, 4H), 2.07 (m, 2H), 1.90 (m, 4H), 1.63−1.37 (m, 20H), 0.88 (t, 3H) (see Figure 1 for details).

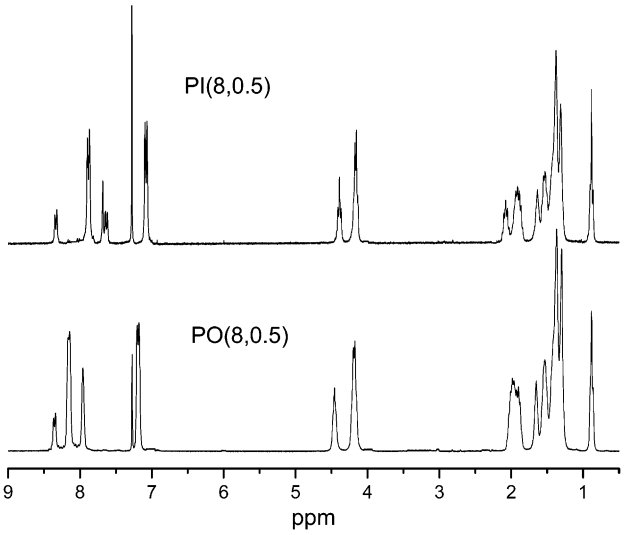

Figure 1. ^{1}H NMR spectra of **PI(8,0.5)** and **PO(8,0.5)** dissolved in deuterated chloroform and trifluoroacetic acid.

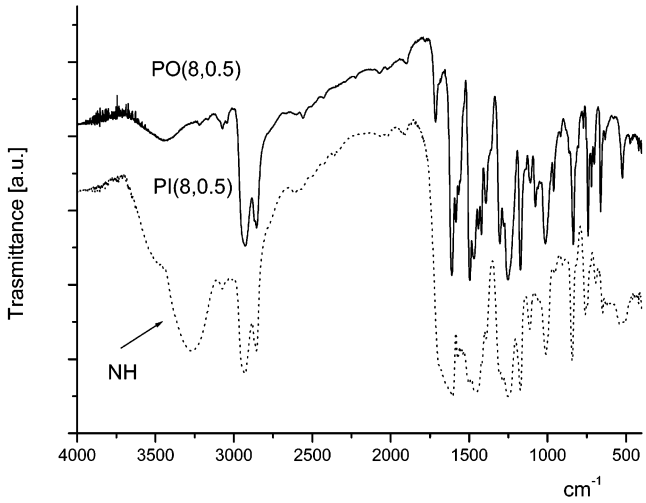

Figure 2. IR spectra of powder samples of **PI(8,0.5)** and **PO-(8,0.5)**.

Scheme 1. Two-Step Synthesis of PO Polymers

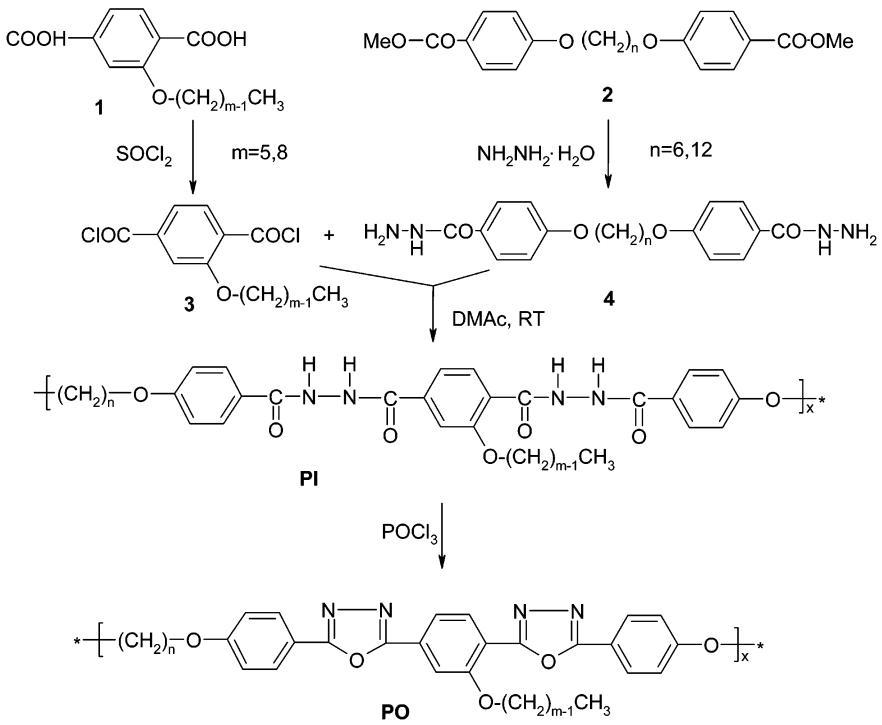

Table 1. Thermodynamic Data of Virgin Samples of PI(*m*,*a*)[a]

PI(*m*,*a*)	T_g (°C)	T_m (°C)	ΔH_m (J/g)	T_{an} (°C)	ΔH_{an} (J/g)	T_{iso} (°C)	ΔH_{iso} (J/g)	T_d (°C)	η_{inh} (dL/g)
PI(5,1)	123.5			231.0	−5.4	235.0	4.4	338.0	0.86
PI(5,0)	105.5			167.0	−4.4	175.4	4.3	343.9	1.00
PI(5,0.5)	120.1			197.3	−4.6	206.0	3.8	331.1	0.75
PI(8,1)	115.8			216.6	−5.6	218.3	4.9	317.2	0.51
PI(8,0)	104.5	202.3	23.7	167.3	−3.2	174.0	2.5	341.7	0.63
PI(8,0.5)	113.7			195.6	−3.7	200.4	3.0	343.6	0.65

[a] T_g = temperature of glass transition; $T_m/\Delta H_m$ = melting temperature/enthalpy, second heating run; $T_{an}/\Delta H_{an}$ = anisotropization temperature/enthalpy, second cooling run; $T_{iso}/\Delta H_{iso}$ = isotropization temperature/enthalpy; T_d = 5% weight loss temperature; η_{inh} = inherent viscosities measured at 25.0 °C in 0.5 g/dL DMF.

Table 2. Thermodynamic Data of Virgin Samples of PO(*m*,*a*)[d]

PO(*m*,*a*)	T_g (°C)	T_m (°C)	ΔH_m (J/g)	T_c (°C)	ΔH_c (J/g)	T_{iso} (°C)	ΔH_{iso} (J/g)	T_d (°C)	η_{inh}[c] (dL/g)
		235.0		223.0					
PO(5,1)	124.5		24.5[a]	210.6	−24.2[a]			365.9	0.35
		224.0		198.3					
				173.7					
PO(5,0)	96.9	211.4	27.6		−25.7[a]			362.5	0.49
				164.6					
PO(5,0.5)	97.3			*168.0/156.0*[b]	*−5.3*[b]	*178.0*[b]	*6.2*[b]	357.4	0.17
		210.0		*203.3*[b]	*−3.35*[b]	*206.4*[b]	*3.2*[b]		
PO(8,1)	116.2		20.2[a]					375.0	0.33
		218.2		178.6	−14.5				
				170.3					
PO(8,0)	105.5	200.0	32.5		−27.5[a]			394.6	0.12
				165.5					
				191.3[b]	*−4.9*[b]	*194.7*[b]	*5.7*[b]		
PO(8,0.5)	101.1	195.7	15.3					380.8	0.39
				136.3	−3.6				

[a] Transition enthalpy, referring to the unresolved set of peaks. [b] Italicized data refer to the reversible nematic-to-isotropic liquid transition. [c] Inherent viscosities were measured at 25.0 °C in 0.5 g/dL chloroform + 5% trifluoroacetic acid solutions, except for the less soluble **PO(5,1)**, which was dissolved in 0.5 g/dL chloroform + 50% trifluoroacetic acid. [d] T_g = temperature of glass transition; $T_m/\Delta H_m$ = melting temperature/enthalpy, second heating run; $T_c/\Delta H_c$ = exothermic transition temperature/enthalpy, second cooling run; $T_{iso}/\Delta H_{iso}$ = isotropization temperature/enthalpy, when resolved; T_d = 5% weight loss temperature.

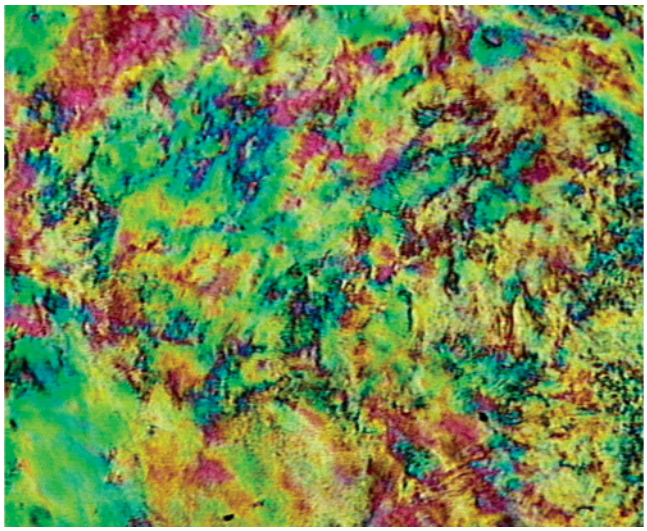

Figure 3. Nematic optical texture of **PI(8,0.5)** taken at 195 °C in the cooling run. Crossed polarizers; 20× magnification.

Step 2: The freshly synthesized polyazide **PI** (1.0 g) was poured into 40 mL of phosphorus oxychloride ($POCl_3$); after 1 h the solution became clear, and the reaction was conducted at the refluxing temperature for 5 h more. The clear solution was cooled and dropped into water (500 mL), to which was added crushed ice and potassium hydrogen carbonate. The precipitate **PO** was filtered and washed with water, dried, and purified by recrystallization from boiling DMAc. The yield is approximately 65%. The proton resonance data are in agreement with the expected values. For example, **PO(8,0.5)** ($CDCl_3/CF_3COOD$): δ (ppm) = 8.35 (d, 1H), 8.16 (d, 4H), 7.96 (m, 2H), 7.19 (d, 4H), 4.46 (t, 2H), 4.18 (m, 4H), 1.95 (m, 6H), 1.65−1.29 (m, 20H), 0.87 (t, 3H) (see Figure 1 for details).

2.2. Characterization. Fibers were extruded from the isotropic phase and cooled to room temperature. The averaged diameter of fibers was 200−300 μm.

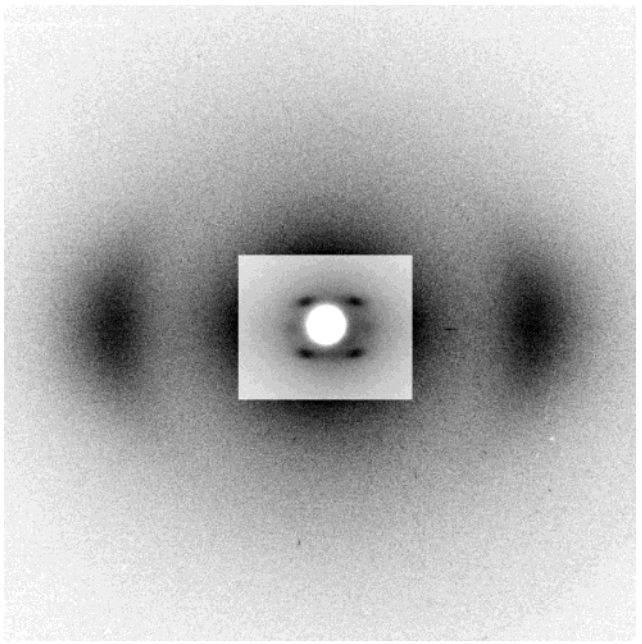

Figure 4. X-ray diffraction pattern recorded at room temperature on a fiber sample of **PI(8,0.5)**. The pattern corresponds to a cybotactic nematic phase.

Thermal measurements were performed by a DSC-7 Perkin-Elmer calorimeter under nitrogen flow at 10 °C/min rate.

Thermogravimetric analysis was performed with a TA Instruments SDT 2960 apparatus, in air at 20 °C/min.

Polarized optical microscopy was performed by a Jenapol microscope fitted with a Linkam THMS 600 hot stage.

An M2000 FTIR spectrometer (by Midac Co.) was adopted to collect IR spectra.

X-ray diffraction spectra were recorded using a flat camera with a sample-to-film distance of 90.0 mm (Ni-filtered Cu Kα

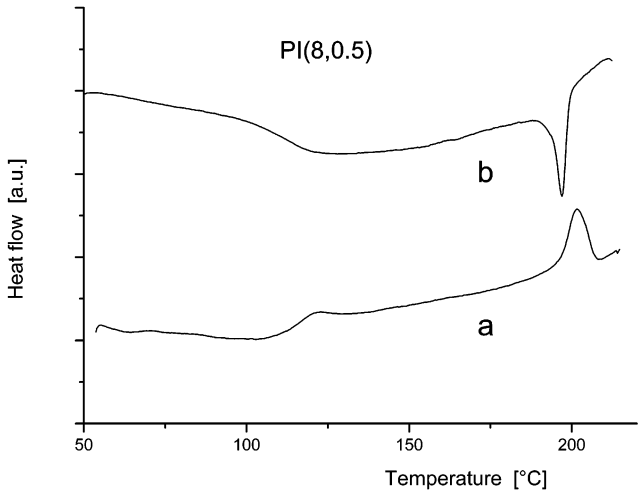

Figure 5. DSC traces of **PI(8,0.5)** powder sample: (a) second heating showing the isotropization transition; (b) first cooling showing the anisotropization transition.

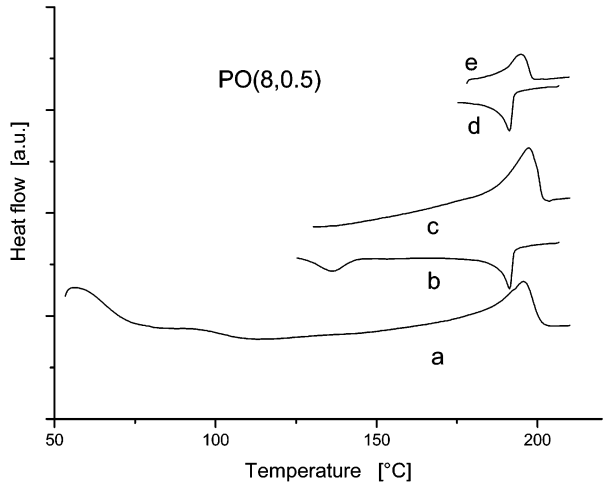

Figure 6. DSC traces of **PO(8,0.5**) powder sample: (a) first heating showing the melting transition; (b) first cooling showing the isotropic liquid-to-nematic transition, followed by the nematic-to-mesophase transition; (c) second heating showing the melting transition; (d, e) cooling run (d) and subsequent fast heating run (e) for isolating the monotropic nematic-to-isotropic liquid transition.

radiation). The Fujifilm MS 2025 imaging plate and a Fuji Bioimaging analyzer system, model BAS-1800, were used for recording and digitizing the diffraction patterns.

^{1}H NMR spectra were recorded with a Bruker DRX/400 spectrometer. Chemical shifts are reported relative to the residual solvent peak.

Inherent viscosities were measured at 25.0 °C with an Ubbelohde viscometer. Viscosities of **PO** were performed in 0.5 g/dL chloroform + 5% trifluoroacetic acid solutions. Viscosities of **PI** were measured in DMF solution.

Films of about 70 μm (evaluated by a KLA-TENCOR P10 surface profiler) have been prepared by spin coating (SET Spinner TP6000 at 1000 rpm rate) from a solution of 3% weight of PO in 1,1,2,2-tetrachloroethane and few drops of trifluoroacetic acid. Films were then dried at 100 °C on a hot plate for 30 min. Under this condition, transparent and amorphous films are obtained.

UV−visible absorption measurements were performed with a Hamamatsu deuterium lamp L2D2 and an Osram HLX Xenophot lamp equipped with two monochromators (a Jobin-Yvon SPEX 1681 monochromator, model 1681B, with a resolution of 0.25 nm, for the incident beam and a Jobin-Yvon ISA TRIAX 320 monochromator, with a resolution of 0.06 nm, for the transmitted beam, respectively). Data were recorded by means of a CCD camera, model MTECCD1024x128−6 (1024 × 128 pixels by 26 μm; spectral range of 200−1000 nm).

Photoluminescence spectra were obtained by means of a Perkin-Elmer LS50 spectrofluorometer on thin films spin coated on quartz glasses (resolution 2.5 nm).

Measurements of polarization dependence on polymer fibers have been performed using, for the excitation, an RLT370-10 highly directional GaN light emitting diode (optical output power of 1 mW; emitting wavelength at 370 nm). For the detection a Spindler and Hoyer polarizer, an UDT-PIN10 silicon photodiode, and a Stanford Research type "SR510" lock-in-amplifier were used.

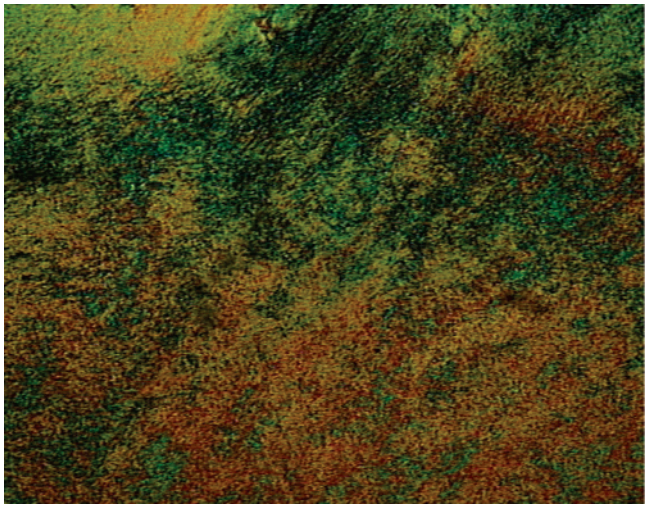

Figure 7. Nematic optical texture of **PO(8,0.5)** taken at 190 °C in the cooling run. Crossed polarizers; 20× magnification.

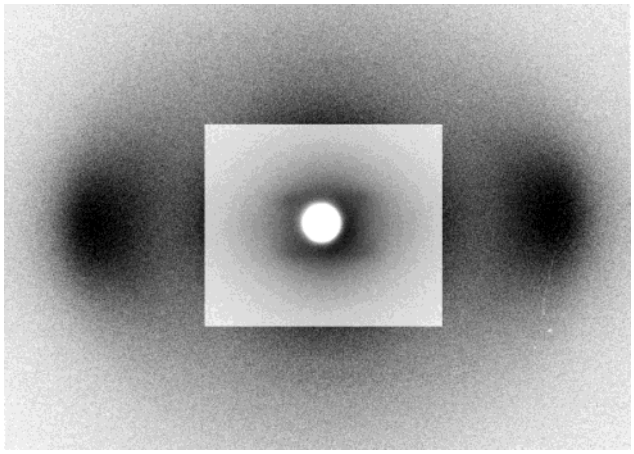

Figure 8. X-ray diffraction pattern of a fiber sample of **PO-(8,0.5)**, taken at room temperature. The pattern corresponds to the quenched nematic phase.

3. Results and Discussion

3.1. Synthesis. The two-steps synthetic path given in Scheme 1 ensures high molecular weights and good quality of final products. This is the consequence of the good solubility of both **PI** and **PO** in $POCl_3$, which avoids the segregation, by precipitation, of the unreacted azide segments along the chain. Consequently, the cyclization is complete according to the ^{1}H NMR spectra (Figure 1) and the disappearing of the characteristic signals of N−H bond (hydrogen bond) in the IR spectra (Figure 2). The single-step procedure based on the direct reaction between the dihydrazide compound **4** and the acid compound **1** in $POCl_3$ was tried, but only oligomeric products were obtained. Moreover the acid compound **1** is low soluble in $POCl_3$, thus the cyclization process is only partial. In the thermogravimetric **PI** trace, a

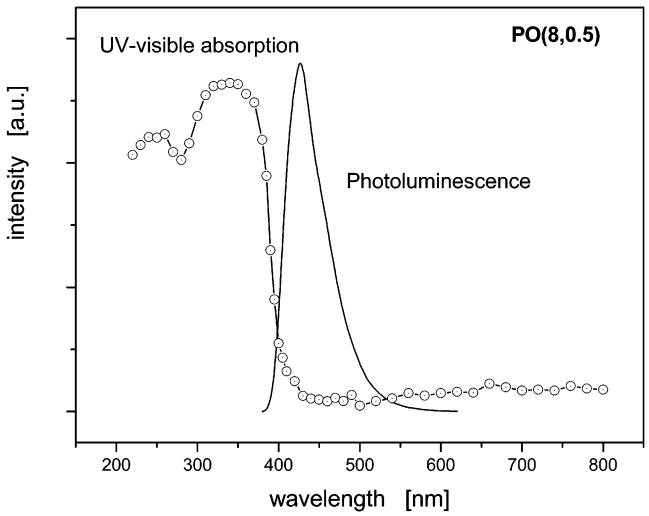

Figure 9. UV−visible absorption and emission spectra of a thin film sample of **PO(8,0.5)**. Emission spectra were recoded by irradiating the sample at 340 nm.

shoulder is observed starting at a temperature of about 290 °C, which corresponds to the loss of water related to the cyclization process (Table 1). **PO** are stable at temperature lower than about 300 °C, while a degradation process occurs at about 320−350 °C, related to thermal decomposition of the less stable aliphatic segments (Table 2).

3.2. Phase Behavior. Thermodynamic properties of **PI** and **PO** polymers are given in Tables 1 and 2, respectively. Hereinafter **PI(8,0.5)** and **PO(8,0.5)** are taken as representative terms of the two series.

PI are liquid crystalline nematic polymers, according to the optical texture shown in Figure 3 and the fluid nature of the anisotropic phase. The X-ray diffraction pattern of a fiber sample of **PI(8,0.5)** recorded at room temperature shows a strong out-meridian reflection at low angle (Figure 4). This reflection, associated with the absence of higher order spots, corresponds to the layerlike packing of chains in a nematic−cybotactic structure (*d*-spacing of 34 Å). The broad halo at high angle corresponds to the chain−chain distance (*d*-spacing of 4.4 Å).

When virgin samples of **PI(8,0.5)** are heated on isotropization, the subsequent cooling and heating traces show only the sharp peak corresponding to the isotropization and to the anisotropization (Figure 5), respectively.

Also **PO** show the nematic phase, but in a monotropic way. According to Table 2, the isotropization transition can be isolated only in the case of **PO(8,1)** and copolymers **PO(5,0.5)**, **PO(8,0.5)**. The flat shape of the conjugated bis(oxadiazole) segment, inserted along the macromolecular chain, promotes the intermolecular packing and, consequently, stabilizes the crystalline phase respect to the nematic phase. In the case of copolymers, the statistical insertion of flexible segments along the chain destabilizes the crystalline order and the nematic phase can be reversibly observed (see Figures 6 and 7).

In a previous paper some of us reported on a class of fully conjugated polymers analogous to **PO** and having the formula[34]

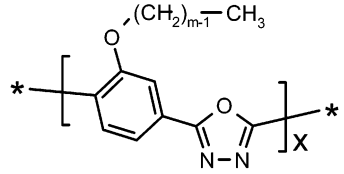

R(m)

R(*m*) do not melt and do not show any liquid crystalline phase. In the case of **PO** the nematic phase is

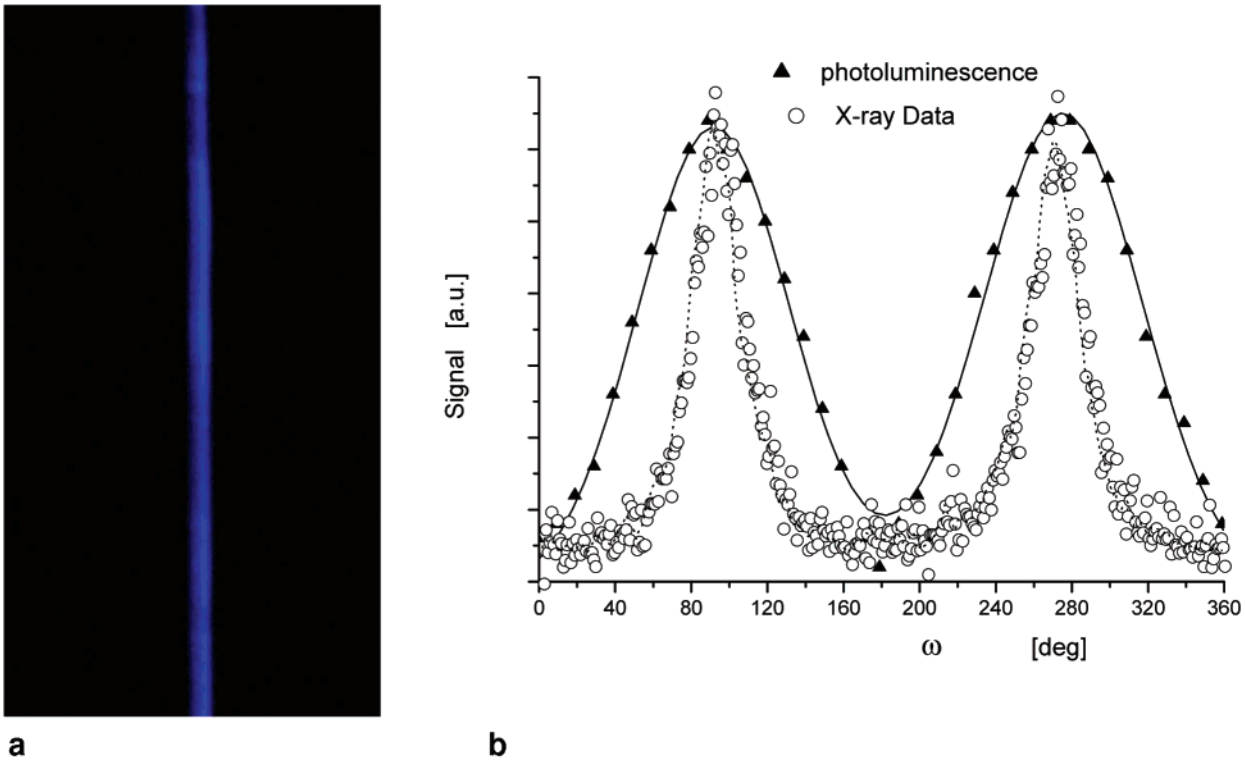

Figure 10. (a) Photoluminescence of **PO(8,0.5)** fiber sample irradiated at 370 nm in the dark. (b) Comparison between the polarized photoluminescence and the polarized X-ray equatorial spot, taken from the pattern shown in Figure 8.

promoted by the combined effects of both the flexible segments inserted along the chain and side ones attached to the chain. In this case, polymers can be extruded from the melt and highly orientated fiber samples can be easily prepared especially in the case of copolymers, taking advantage of the nematic nature of the molten phase (see Figure 8).

3.3. Optical Properties and Photoluminescence. As already pointed out, the use of the oxadiazole frame in the synthesis of new materials, suitable for the fabrication of OLED, has been widely investigated. The main reason is the possibility to extend the electron-transport character of this molecular frame to new materials and to set emission in the blue region of the visible spectra.

Polymers **PO** are quite transparent in the visible range and strongly absorb in the UV range as shown in Figure 9. There are two strong and broad absorption bands peaked at about 340 and 250 nm, which obviously depends only on the oxadiazole moiety and is independent of the aliphatic insertions.

When film samples are exposed to UV radiation, **PO** show a strong photoluminescence in the blue region of the spectrum. When a sample is irradiated at 340 nm, the emission spectrum shows a broad peak located at about 430 nm with a shoulder at about 460 nm (Figure 9), similar to that reported for analogous oxadiazole-containing compounds.

PO copolymers can be easily extruded to give oriented fiber samples due to the nematic nature of the material. The consequence is the parallel packing of chains in a macrodomain. The reciprocal alignment of the oxadiazole units in a macroscopic array influences the response to the UV irradiation in the two directions parallel and perpendicular to the fiber axis, respectively. As a consequence, polymers give in emission a polarized photoluminescence (see Figure 10) with the same period of the X-ray diffraction. Compared to the polarization of the nematic halo in the diffraction pattern shown in Figure 8, photoluminescence profile is broader as consequence of the scatter due to sample anisotropy.

4. Conclusions

According to our previous contribution about low molecular mass compounds containing oxadiazole unit[32] and to several reports on similar systems,[19,24−31] **PO** are blue photoluminescent materials. Taking advantage of the nematic phase, **PO** can be easily oriented to make fiber samples from the molten state. Oriented samples emit polarized photoluminescence.

Thanks to the flexible spacers along the chain and the side pendant segments, **PO** are soluble in common chlorinate solvents. Thin films obtained by spinning technique show strong emission in the blue region of the visible spectra.

All these features make **PO** suitable to be used as active material in the fabrication of blue-emitting OLED. The study of electronic properties of **PO** and the realization of an electroluminescent device using **PO** as the electron transport component are under scrutiny.

Acknowledgment. Support by FIRB "Micropolys" Project financed by the Ministero dell'Istruzione, dell'Università e della Ricerca (MIUR) is gratefully acknowledged.

References and Notes

(1) Burroughes, J. H.; Bradley, D. D. C.; Brown, A. R.; Marks, R. N.; Mackay, K.; Friend, R. H.; Burns, P. L.; Holmes, A. B. *Nature (London)* **1990**, *347*, 539.
(2) Holmes, A. B.; Bradley, D. D. C.; Brown, A. R.; Burn, P. L.; Burroughes, J. H.; Frien, R. H.; Greenham, N. C.; Gymer, R. W.; Halliday, D. A.; Jackson, R. W.; Kraft, A.; Martens, J. H. F.; Pichler, K.; Samuel, I. D. W. *Synth. Met.* **1993**, *55−57*, 4031.
(3) Berggren, M.; Inganäs, O.; Gustafsson, G.; Rasmusson, J.; Andersson, M. R.; Hijertberg, T.; Wennerstrom, O. *Nature (London)* **1994**, *372*, 444.
(4) Brown, B.; Bradley, D. D. C.; Burroughs, J. H.; Friend, R. H.; Greenham, N. C.; Burn, P. L.; Holmes, A. B.; Kraft, A. *Appl. Phys. Lett.* **1992**, *61*, 2793.
(5) Grem, G.; Leditzky, G.; Ulrich, B.; Leising, G. *Adv. Mater.* **1992**, *4*, 36.
(6) Adachi, C.; Tsutsui, T.; Saito, S. *Appl. Phys. Lett.* **1990**, *56*, 799.
(7) Hedrick, J. L.; Tweig, T. *Macromolecules* **1992**, *25*, 2021.
(8) Strukelj, M.; Papadimitrakopoulos, F.; Miller, T. M.; Rothberg, L. J. *Science* **1995**, *267*, 1969.
(9) Li, X. C.; Holmes, A. B.; Kraft, A.; Moratti, S. C.; Spencer, G. C. W.; Cacialli, F.; Grüner, J.; Friend, R. H. *J. Chem. Soc., Chem. Commun.* **1995**, 2211.
(10) Li, X. C.; Spencer, G. C. W.; Holmes, A. B.; Moratti, S. C.; Cacialli, F.; Friend, R. H. *Synth. Met.* **1996**, *76*, 153.
(11) Pei, Q.; Yang, Y. *Chem. Mater.* **1995**, *7*, 1568.
(12) Buchwald, R.; Meier, M.; Karg, S.; Pösch, P.; Schmidt, H. W.; Strohriegl, P.; Riess, W.; Schwoerer, M. *Adv. Mater.* **1995**, *7*, 839.
(13) Huang, W.; Yu, W. L.; Meng, H.; Pei, J.; Li, S. F. Y. *Chem. Mater.* **1998**, *10*, 3340.
(14) Lee, J. I.; Klaerner, G.; Miller, R. D. *Chem. Mater.* **1999**, *11*, 1083.
(15) Li, X. C.; Liu, Y.; Liu, M. S.; Jen, A. K. J. *Chem. Mater.* **1999**, *11*, 1568.
(16) Liu, Y.; Liu, M. S.; Li, X. C.; Jen, A. K. J. *Chem. Mater.* **1998**, *10*, 3301.
(17) Liu, Y.; Ma, H.; Jen, A. K. J. *Chem. Mater.* **1999**, *11*, 27.
(18) Peng, Z.; Zhang, J. *Chem. Mater.* **1999**, *11*, 1138.
(19) Bao, Z.; Peng, Z. *Chem. Mater.* **1998**, *10*, 1202.
(20) Lu, J.; Hlil, A. R.; Sun, Y.; Hay, A. S.; Maindron, T.; Dodelet, J. P.; D'Iorio, M. *Chem. Mater.* **1999**, *11*, 2501.
(21) Casu, M. B.; Imperia, P.; Schrader, S.; Schulz, B.; Jandke, M.; Strohriegl, P. *Synth. Met.* **2001**, *121*, 1397.
(22) Xu, B.; Pan, Y.; Zhang, J.; Peng, Z. *Synth. Met.* **2000**, *114*, 337.
(23) Wang, Z.; Yang, X.; Chen, X.; Xu, Z.; Xu, X. *Thin Solid Films* **2000**, *363*, 94.
(24) Meier, M.; Buchwald, E.; Karg, S.; Pösch, P.; Greczmiel, M.; Strohriegl, P.; Riess, W. *Synth. Met.* **1996**, *76*, 95.
(25) Paik, K. L.; Baek, N. S.; Kim, H. K.; Lee, J. H.; Lee, Y. *Opt. Mater.* **2002**, *21*, 135.
(26) Jousseaume, V.; Maindron, T.; Wang, Y.; Dodelet, J. P.; Lu, J.; Hlil, A. R.; Hay, A. S.; D'Iorio, M. *Thin Solid Films* **2002**, *416*, 201.
(27) Ding, J.; Tao, Y.; Day, M.; Roovers, J.; D'Iorio, M. J. *Opt. A: Pure Appl. Opt.* **2002**, *4*, S267.
(28) Zheng, S.; Shi, J. *Chem. Mater.* **1999**, *13*, 4405.
(29) Paik, K. L.; Baek, N. S.; Kim, H. K.; Lee, Y.; Lee, K. J. *Thin Solid Films* **2002**, *417*, 132.
(30) Song, S. Y.; Jang, M. S.; Shim, H. K.; Song, L. S.; Kim, W. H. *Synth. Met.* **1999**, *102*, 1116.
(31) Bettenhausen, J.; Greczmiel, M.; Jandke, M.; Strohriegl, P. *Synth. Met.* **1997**, *91*, 223.
(32) Li, X. C.; Spencer, G. C. W.; Holmes, A. B.; Moratti, S. C.; Cacialli, F.; Friend, R. H. *Synth. Met.* **1996**, *76*, 153.
(33) Acierno, D.; Concilio, S.; Diodati, A.; Iannelli, P.; Piotto Piotto, S.; Scarfato, P. *Liq. Cryst.* **2002**, *29*, 1383.
(34) Caruso, U.; Iannelli, P.; Roviello, A.; Sirigu, A. *J. Polym. Sci., Polym. Phys.* **1997**, *36*, 2371.
(35) Gillo, M.; Iannelli, P.; Laurienzo, P.; Malinconico, M.; Roviello, A.; Mormile, P.; Petti, L. *Chem. Mater.* **2002**, *14*, 1539.

MA034382F